

METTL3/YTHDF2 m6A axis promotes the malignant progression of bladder cancer by epigenetically suppressing RRAS

JIE-XUN CHEN*, DONG-MING CHEN*, DONG WANG, YI XIAO, SHUAI ZHU and XIAN-LIN XU

Department of Urology, Sir Run Run Hospital, Nanjing Medical University, Nanjing, Jiangsu 210008, P.R. China

Received October 17, 2022; Accepted March 9, 2023

DOI: 10.3892/or.2023.8531

Abstract. The present study aimed to explore the potential roles of the methyltransferase-like 3 (METTL3)-mediated methylation of RAS related (RRAS) mRNA in the tumorigenesis and development of bladder cancer (BCa). For this purpose, the relative expression levels of METTL3 in BCa specimens and cell lines were measured using reverse transcription-quantitative PCR (RT-qPCR) and western blot analysis. The association between the METTL3 expression level and the clinical characteristics of patients with BCa was analyzed using The Cancer Genome Atlas (TCGA) and Gene Expression Profiling Interactive Analysis databases. Cellular experiments were performed to confirm the effects of METTL3 on the proliferative, migratory and invasive capacities of BCa cells. RT-qPCR, western blot analysis, methylated RNA immunoprecipitation (MeRIP)-qPCR and dual-luciferase report assays were utilized to verify the METTL3/RRAS/YTH N⁶-methyladenosine (m6A) RNA binding protein 2 (YTHDF2) regulatory axis in BCa. The results revealed that METTL3 expression was markedly increased in BCa specimens and cell lines, and was associated with poor clinical characteristics of patients with BCa. *In vitro* and *in vivo* assays demonstrated that the silencing of METTL3 markedly suppressed the proliferative, migratory and invasive capacities of BCa cells. MeRIP-PCR and dual-luciferase report assays indicated that METTL3 could bind to the m6A sites of RRAS mRNA and suppress the transcriptional activity of RRAS. YTHDF2 could recognize the m6A sites of RRAS and mediate RRAS degradation. On the whole, the findings of the present study reveal the pivotal role of METTL3-catalyzed

m6A modification in BCa tumorigenesis and development. The change could facilitate BCa tumor growth and metastasis by suppressing RRAS expression in an m6A YTHDF2-dependent manner. Targeting the METTL3/RRAS/YTHDF2 regulatory axis may thus prove to be a promising strategy for the diagnosis and therapy of BCa.

Introduction

Bladder cancer (BCa) is one of the most common urological cancers. The most common histologic type of BCa is uroepithelial carcinoma, which accounts for ~95% of cases (1,2). Since the cancer cells originate from the metastatic epithelium of the bladder, it is also known as metastatic cell carcinoma. Based on the depth of tumor infiltration, BCa can be classified as non-muscle-invasive BCa (NMIBC, ~75% of cases) and muscle-invasive BCa (MIBC; ~25% of cases) (3). NMIBC is usually treated conservatively, which preserves bladder structure and function. Progression or recurrence can be prevented by transurethral resection followed by intravesical instillation (4). However, recurrence can occur in >50% of patients with NMIBC; of these cases, 10 to 30% progress to MIBC or even metastasis (5). MIBC is highly malignant, has a rapid disease progression, and is characterized by metastasis and recurrence (6). The main treatment options for MIBC are radical surgery and radiotherapy; 25% of patients with MIBC have a poor prognosis (7,8). In addition, the existing diagnostic methods for BCa, such as cystoscopy and urine cytology, are invasive procedures that can lead to patient discomfort or are costly and have a poor sensitivity (9). Therefore, clarifying the underlying pathogenesis of BCa and identifying biomarkers that accurately identify early cases are urgent research goals.

A number of studies have verified that monomethylated (m) modifications on the sixth nitrogen atom of adenine (A) of RNA (designated as m6A) are essential in tumor development. m6A modifications usually occur in a variety of RNAs, including messenger RNAs (mRNAs), long non-coding RNAs (lncRNAs), circular RNAs, small nuclear RNAs, transfer RNAs and ribosomal RNAs (10,11). m6A modification sites are highly conserved and tend to appear on the common sequence RR m6ACH (R=G/A, H=A/C/U), which are mainly located near the 3' untranslated repeat, stop codon, or long exon of RNA. The sites are crucial for the splicing of RNA precursors, 3' end processing, extranuclear transport, degradation and translation (12). The m6A modification is reversible. Its

Correspondence to: Dr Shuai Zhu or Dr Xian-Lin Xu, Department of Urology, Sir Run Run Hospital, Nanjing Medical University, 109 Longmian Avenue, Jiangning, Nanjing, Jiangsu 210008, P.R. China
E-mail: zhushuai@163.com
E-mail: xianlinxu@njmu.edu.cn

*Contributed equally

Key words: N⁶-methyladenosine, bladder cancer, RAS related, methyltransferase-like 3, malignant progression

regulation is dynamic and consists of methyltransferase (writer), demethylase (eraser) and methyl recognition protein (reader), which perform different functions (13,14). Methylation enzymes catalyze the methylation of the target. The enzymes are m(6)A methyltransferase (METTL3), METTL14 and Wilms' tumor 1-associating protein (WTAP), which form the METTL3/METTL14/WTAP complex (15). Demethylases catalyze demethylation. With the involvement of ferrous ion (Fe^{2+}) and α -ketoglutarate, m6A methylation can be cleared by fat mass and obesity-associated protein and AlkB homolog 5, RNA demethylase (ALKBH5) (16). The demethylase readers, including YTH N⁶-methyladenosine RNA binding protein 3 (YTHDF1-3), YTHDC1-2, eukaryotic initiation factor 3, heterogeneous nuclear ribonucleoproteins, HUR and insulin-like growth factor-2 mRNA-binding proteins (IGF2BPs) can recognize methylation information (17). As a result, m6A is involved in a closed-loop, reversible process that regulates its own methylation level and the expression of upstream and downstream related genes.

METTL3 is the most common and most extensively studied methyltransferase of m6A. m6A modifications significantly modulate RNA stability, localization, transport, splicing and translation (18). METTL3 also plays an integral role in the development and progression of various of tumors. METTL3 promotes homologous recombination repair through the regulation of the EGF/RAD51 signaling axis, thereby regulating the chemotherapeutic response in breast cancer (19). METTL3 mediates the m6A modification of six-transmembrane epithelial antigen of the prostate-2 (STEAP2) and promotes the malignant progression of papillary thyroid cancer by inhibiting the Hedgehog signaling pathway and epithelial-mesenchymal transition (20). METTL3 can promote poly(ADP-ribose) polymerase 1 mRNA stability and thus resistance to oxaliplatin in CD133⁺ stem cells of gastric cancer (21). In addition, METTL3 is also involved in the carcinogenesis and progression of BCa. c-Jun N-terminal kinase (JNK) signaling promotes immune escape from BCa by modulating the METTL3-mediated m6A modification of programmed death-ligand 1 (PD-L1) (22). METTL3 can promote the malignant progression of BCa by regulating the ALF transcription elongation factor 4/nuclear factor- κ B/MYC signaling network (23). METTL3 can accelerate the maturation of pri-microRNA (miRNA/miR)-221/miR-222 and can thus promote the proliferation of BCa cells in an m6A-dependent manner (22). However, the specific biological effects and molecular mechanisms of METTL3 in BCa need to be further explored.

The present study detected the expression level of METTL3 in BCa tissues and cell lines, and validated the biological role of METTL3 in BCa. In addition, the role of the METTL3/RAS related (RRAS)/YTHDF2 regulatory axis in the tumorigenesis and development of BCa was examined. The collective findings may provide a theoretical basis for the comprehensive clinical diagnosis and treatment of BCa.

Materials and methods

Bioinformatics analysis. The expression levels of METTL3 in BCa were analyzed by utilizing the UANAL database (<http://ualcan.path.uab.edu/>). In The Cancer Genome Atlas

(TCGA), urothelial bladder carcinoma (BLCA) data were selected, METTL3 was entered, and the Expression function was selected to analyze the association of METTL3 expression levels with sample types, individual cancer stages and nodal metastasis status. The Gene Expression Profiling Interactive Analysis 2 (GEPIA2) visual network analysis tool (<http://gepia2.cancer-pku.cn/>) was utilized for the analysis. Survival analysis utilized BLCA data. METTL3 was entered, the Group Cut-off was median, and Axis Units were months. The high and low group was depicted in red and blue, respectively, and survival curves were plotted.

Specimen collection. A total of 40 BCa tissues and para-cancerous tissues were obtained from specimens surgically resected from bladder cancer at the Department of Urology, Sir Run Run Hospital, Nanjing Medical University from January, 2019 to December, 2021. The inclusion and exclusion criteria for the selection of patients with BCa are listed in Table SI. None of the patients had been treated with radiotherapy and chemotherapy prior to surgery. All tissue specimens were identified by two or more pathologists. Ethics approval was provided by the Ethics Committee of Sir Run Run Hospital, Nanjing Medical University (2019-SR-S019). All patients provided signed informed consent and agreed to the publication of their data.

Cells, cell culture and transfection. Normal control (NC) cells (SV-HUC-1) (cat. no. TCHu169) and the BCa cell lines, UM-UC-3 (cat. no. TCHu217), T24 (cat. no. TCHu 55), J82 (cat. no. TCHu218), TCCSUP (cat. no. SCSP-571) and 5637 (cat. no. TCHu 1), were obtained from The Cell Bank of Type Culture Collection of the Chinese Academy of Sciences. The UM-UC-3 and SV-HUC-1 cells were cultured in Dulbecco's modified Eagle's medium (Gibco; Thermo Fisher Scientific, Inc.) supplemented with 10% fetal bovine serum and 2% double antibiotics (Gibco; Thermo Fisher Scientific, Inc.). The T24, J82, TCCSUP and 5637 cells were cultured in RPMI-1640 medium (Gibco; Thermo Fisher Scientific, Inc.) supplemented with 10% fetal bovine serum and 2% double antibiotics (Gibco; Thermo Fisher Scientific, Inc.) at 37°C in a 5% CO₂ atmosphere. Both the T24 and J82 cells were cultured to 80% confluency, and transfection was performed with a concentration of 2.5 μ g overexpression plasmids (OE)-Vector (or OE-METTL3, OE-RRAS and OE-YTHDF2) and 30 nM small interfering RNA (siRNA)-NC (or si-METTL3 and si-YTHDF2) in six-well plates at 1x10⁵ cells/well using Lipofectamine™ 2000® Transfection Reagent (Invitrogen; Thermo Fisher Scientific, Inc.) according to the manufacturer's instructions at 37°C for 48 h. The time interval between transfection and subsequent experimentation was 48 h. After the transfection efficiency was verified using reverse transcription-quantitative PCR (RT-qPCR) and western blot analysis, the experiments were performed. All the siRNAs and overexpression plasmids were purchased from Shanghai GeneChem Co., Ltd. The siRNA sequences are presented in Table SII.

Lentiviruses and infection. The lentiviral vectors (LV)-small hairpin RNA (shRNA) based on a third generation lentiviral system targeting METTL3 (LV-shMETTL3) and negative

control (LV-shNC) were purchased from Shanghai GeneChem Co., Ltd. Briefly, 2.0 μg shRNA vector and 2.0 μg packaging mix plasmids were transfected into 293T cells (cat. no. C6008; Beyotime Institute of Biotechnology) using Lipofectamine 3000[®] reagent (Thermo Fisher Scientific, Inc.) for 24 h at 37°C, and the medium was then harvested and the virus was extracted by 85,000 \times g ultracentrifugation at 4°C for 2 h in a centrifuge (Beckman Coulter, Inc.). For lentiviral transduction, the cells were seeded in six-well plates at a density of 50,000 cells/well. The lentiviral vector was added at a multiplicity of infection of 20, with 8 μg polybrene (Sigma-Aldrich; Merck KGaA) per well. After 72 h, the cells infected with the lentiviral vectors were selected using puromycin (Beyotime Institute of Biotechnology). The concentration of puromycin used for selection was 2 $\mu\text{g}/\text{ml}$, and the concentration used for maintenance was 1 $\mu\text{g}/\text{ml}$. The knockdown efficiency was evaluated using RT-qPCR.

RNA extraction and RT-qPCR. Total RNA was extracted from the BCa tissues and cells using TRIzol[®] reagent (Life; Thermo Fisher Scientific, Inc.) and the RNA concentration was detected. Complimentary DNA (cDNA) was synthesized by the reverse transcription of RNA in accordance with the instructions provided with the kit (Takara Bio, Inc.). The cDNA was diluted 20 times for RT-qPCR. qPCR was performed according to the instructions provided with the SYBR Green mix kit (Takara Bio, Inc.). The reaction conditions were 95°C for 2 min and 30 cycles of 95°C for 30 sec, 58°C for 30 sec, and 72°C for 30 sec. glyceraldehyde 3-phosphate dehydrogenase (GAPDH) were used as internal references. The qPCR fluorescence values were calculated using the $2^{-\Delta\Delta C_q}$ method (24). The primers used are listed in Table SIII.

Cell counting kit-8 (CCK-8) assay. The transfected BCa cells were inoculated in wells of 96-well plates (3,000 cells per well). Following 24 h of cell culture, 10 μl CCK-8 reagent (Dojindo Laboratories, Inc.) was added to each well and incubation was continued at 37°C in a 5% CO₂ incubator protected from light. After 2 h, the absorbance of each well was measured at 450 nm. The results were compared using an unpaired t-test with GraphPad 7.0 software (GraphPad Software Inc.).

5-ethynyl-2'-deoxyuridine (EdU) assay. Following transfection for 48 h, single cell suspensions were prepared from each group of cells in good condition at the logarithmic growth stage. Wells of 96-well plates were inoculated with 5 \times 10³ cells/well. Cell proliferation was assessed using the EdU kit (Guangzhou RiboBio Co., Ltd.). A total of 50 mM EdU solution was added to the BCa cells and incubated for at 37°C for 2 h. Following incubation, the cells were fixed with 4% paraformaldehyde at 20°C for 15 min, treated with 0.1% Triton X-100 at 20°C for 5 min, closed with 5% bovine serum albumin (Invitrogen; Thermo Fisher Scientific, Inc.) for 30 min at 20°C, removed from the cell crawl and washed. Rhodamine (Merck Co., Ltd.) was added and the cells were incubated with the EdU reaction mixture for 20 min at 20°C. The nuclei were re-fixed with Hoechst for 15 min at 20°C. Images were captured under a fluorescent microscope at x200 magnification (Olympus Corporation) to calculate cell proliferation using ImageJ software (Version 1.45s; National Institutes of Health).

Transwell assay. The transfected BCa cells (\sim 2 \times 10⁵ cells/ml) were inoculated in the upper chamber (200 μl /well) of a Transwell device (Corning, Inc.). The lower chamber was incubated with culture medium containing 10% fetal bovine serum (60 μl /well) and incubated for 24 h at 37°C. The cells were washed with PBS, fixed by the addition of paraformaldehyde for 20 min at 20°C, and stained with 0.1% crystal violet (Beyotime Institute of Biotechnology) for 10 min at 20°C. The number of migrating cells was observed under a fluorescent microscope (Olympus Corporation) for 10 min. For the Transwell invasion assay, the pre-cooled culture medium was used to dilute the Matrigel matrix (0.8 μm ; Corning, Inc.) gel, which was added to the upper chamber and incubated for 5 h at 37°C. The BCa cell suspension was then added, and the subsequent experimental steps were the same as those for the cell migration assay. The number of invading cells was determined under a fluorescent microscope (Olympus Corporation). Images were captured under a fluorescent microscope at x200 magnification (Olympus Corporation) to calculate cell migration and invasion using ImageJ software (Version 1.45s; National Institutes of Health).

Cell cycle analysis. The transfected BCa cells were cultured in six-well plates for 48 h and then digested and resuspended. Following centrifugation x1,500 g at 4°C for 10 min, the supernatant was discarded and the cells were suspended in 75% ethanol at 4°C and fixed overnight. Propidium iodide (PI) staining solution (Merck Co., Ltd.) was added to each tube (0.5 ml) after subsequent washing, mixed well and incubated in an incubator at 37°C for 30 min protected from light, followed by automated detection at 4°C. Cell cycle localization at each stage was measured using the FACSCanto II flow cytometer (BD Biosciences) at a wavelength of 488 nm and the data were analyzed using BD FACSDiva Software version 8.0.2 (BD Biosciences).

Cell apoptosis analysis. The transfected BCa cells were cultured in six-well plates for 48 h. The cells were then digested, resuspended and transferred to 15-ml centrifuge tubes. Following centrifugation x1,500 g at 4°C for 15 min, the supernatant was removed and 195 μl fluorescein isothiocyanate (FITC) conjugate (Merck Co., Ltd.) was added to each Eppendorf tube (Merck Co., Ltd.). The cells were resuspended, followed by the sequential addition of 5 μl FITC and 10 μl PI staining (Merck Co., Ltd.) solution. The contents were mixed well and left static for 30 min at room temperature protected from light, and then transferred to a refrigerator at 4°C. The cells were incubated for 30 min at room temperature and then transferred to a refrigerator at 4°C. Cellular apoptosis was detected on a FACSCanto II flow cytometer (BD Biosciences), and the data were analyzed with BD FACSDiva Software version 8.0.2 (BD Biosciences).

Western blot analysis. Protein extracts were prepared by cell lysis using radioimmunoprecipitation assay buffer (RIPA, Beyotime Institute of Biotechnology). The protein concentration was determined using a BCA protein assay kit (Beyotime Institute of Biotechnology), and 20 mg protein extract were separated by 10% sodium dodecyl sulfate-poly-acrylamide gel electrophoresis (SDS-PAGE)

followed by transfer onto a polyvinylidene fluoride (PVDF) microporous membranes (MilliporeSigma). The PVDF membranes were blocked by placing them in Tris-buffered saline containing 0.1% Tween-20 and blocked with 5% non-fat milk at room temperature for 2 h and incubated with rabbit primary antibodies against METTL3 (1:1,000, cat. no. ab195352), GAPDH (1:3,000, cat. no. ab181602), YTHDF2 (1:1,000, cat. no. ab246514) and RRAS (1:1,000, cat. no. ab154962) (all from Abcam) at 4°C for 12 h. The PVDF membranes were incubated with HRP-conjugated Affinipure goat anti-mouse IgG (H+L) (1:10,000; cat. no. SA00001-1; ProteinTech Group, Inc.) or HRP-conjugated Affinipure goat anti-rabbit IgG (H+L) (1:10,000; cat. no. SA00001-2; ProteinTech Group, Inc.) at room temperature for 2 h. The western blot bands were visualized using an ECL Kit (Vazyme Biotech Co., Ltd.) and images were captured using the Tanon 4600 system (Tanon Science and Technology Co., Ltd.). Finally, ImageJ software (version 1.45s; National Institutes of Health) was used to calculate the relative gray value.

m6A-RNA immunoprecipitation assay. Total RNA (100 µg) was pre-cleared by incubation with 20 µl recombinant protein-G sepharose bead suspension (Invitrogen; Thermo Fisher Scientific, Inc.) in Magna Methylated RNA Immunoprecipitation (MeRIP) buffer (10 mM Tris-HCl, pH 7.5, 150 mM NaCl, 0.1% NP-40, 2 mM ribonucleoside vanadyl complexes and 200 U/ml RNasin) for 1 h at 4°C according to the manufacturer's instructions. The pre-cleared RNA was incubated with 1 µg anti-m6A antibody (cat. no. ab286164, Abcam) for 4 h at 4°C. Recombinant protein-G sepharose beads (50 µl) were blocked using 0.5 mg/ml bovine serum albumin in meRIP buffer for 1 h at 4°C. The RNA-antibody mixture was incubated with the pre-cleared beads and for 2 h at 4°C. The beads were then washed five times with the meRIP buffer, and the mRNA bound to the beads was eluted using 100 µl elution buffer (meRIP buffer supplemented with 6.7 mM N6-methyladenosine base; Selleck Chemicals) at 4°C for 1 h. The fragmented RNA containing m6A was eluted and purified using the RNA purification kit (Qiagen, Inc.). The enriched fragments were analyzed using RT-qPCR.

RNA binding protein immunoprecipitation (RIP) assay. RIP experiments were performed using the Magna RIP kit (MilliporeSigma) according to the instructions provided by the manufacturer. Briefly, the cells (1×10^7 cells per 150 µl) were collected and lysed in a complete radioimmunoprecipitation assay buffer containing a protease inhibitor cocktail and RNase inhibitor. Magnetic beads coated with 5 µg specific antibodies against mouse IgG (SAB5600281, MilliporeSigma, Merck Co., Ltd.) or YTHDF2 (1/30, ab220163, Abcam) were pre-bound to protein A/G magnetic beads in immunoprecipitation buffer (20 mM Tris-HCl pH 7.5, 140 mM NaCl, 0.05% Triton X-100) (MilliporeSigma, Merck Co., Ltd.) for 2 h and then incubated with 100 µl cell lysate overnight at 4°C with rotation. RNA was eluted from the beads by incubation with 400 µl elution buffer for 2 h, precipitated with ethanol and dissolved in RNase-free water. The enrichment of certain fragments was determined using RT-qPCR.

Luciferase reporter gene assay. DNA fragments containing the wild-type or mutant CDS region of RRAS were inserted into the pmirGLO plasmids (GeneChem Co., Ltd.). Plasmids (2 µg) containing the wild-type or mutant fragments of the RRAS CDS region were co-transfected into 293T cells with METTL3 overexpression plasmids (2 µg) or NC using Lipofectamine 3000® reagent (Thermo Fisher Scientific, Inc.). Following 48 h of transfection, analysis was performed using a dual-luciferase reporter gene analysis system (Promega Corporation). The ratio of Firefly luciferase signal to the *Renilla* luciferase signal was calculated to evaluate the modification effect of METTL3 on m6A of RRAS.

Xenograft experiments. The animal experiment was approved (approval no. 2021-AR-008) and monitored by the Animal Ethics Committee of Sir Run Run Hospital, Nanjing Medical University. A total of 16 male, 4- to 6-week-old BALB/c nude mice weighing 18-26 g, were purchased from the Institute of Model Animals, Nanjing University and raised in a specific pathogen-free (SPF) environment for the xenograft model. The mice were raised in animal individually ventilated cage (IVC cages) with a room temperature of 24°C and relative humidity of 70% and the air exchange rate was 15 times/h. The mice could drink filtered tap water and commercial feed *ad libitum* under a strict 12-h light/dark cycle. The animal laboratory was cleaned twice one day and sterilized with ultraviolet light for 1 h each week. Each mouse was injected with 100 µl PBS containing 1×10^6 T24 cell lines expressing either LV-NC or LV-shMETTL3 subcutaneously under the right armpit. Tumor volumes were recorded on day 7 after the injection and then measured each week. At day 28, the mice were sacrificed by cervical dislocation following the inhalation of 3% isoflurane anesthesia and the death of the mice was confirmed by respiratory arrest. Tumor weights were also compared. The data from each group of mice are expressed as the mean ± standard deviation (SD).

Statistical analysis. Each experiment was independently repeated in triplicate. GraphPad Prism 8.0 (GraphPad Software Inc.) and SPSS 22.0 (IBM Corp.) were used for data analysis. The data are presented as mean ± SD. The data from two groups were compared using an unpaired t-test. Differences between three or more groups were evaluated using a one-way ANOVA multiple comparison test, followed by Tukey's post hoc test. Pearson's correlation analysis was performed to assess the correlations between genes. A P-value <0.05 was considered to indicate a statistically significant difference.

Results

METTL3 is significantly overexpressed in BCa. To verify the expression level of METTL3 in BCa, the GEPIA database was first used for analysis. The expression level of METTL3 was significantly higher in BCa tissues than in normal control tissues (Fig. 1A). The association between the METTL3 expression levels and BCa cancer stages and nodal metastasis status was also analyzed using TCGA data. The results revealed that a high expression level of METTL3 was positively associated with BCa cancer stages and nodal metastasis (Fig. 1B and C). Subsequently, the association between the METTL3 expression levels and the

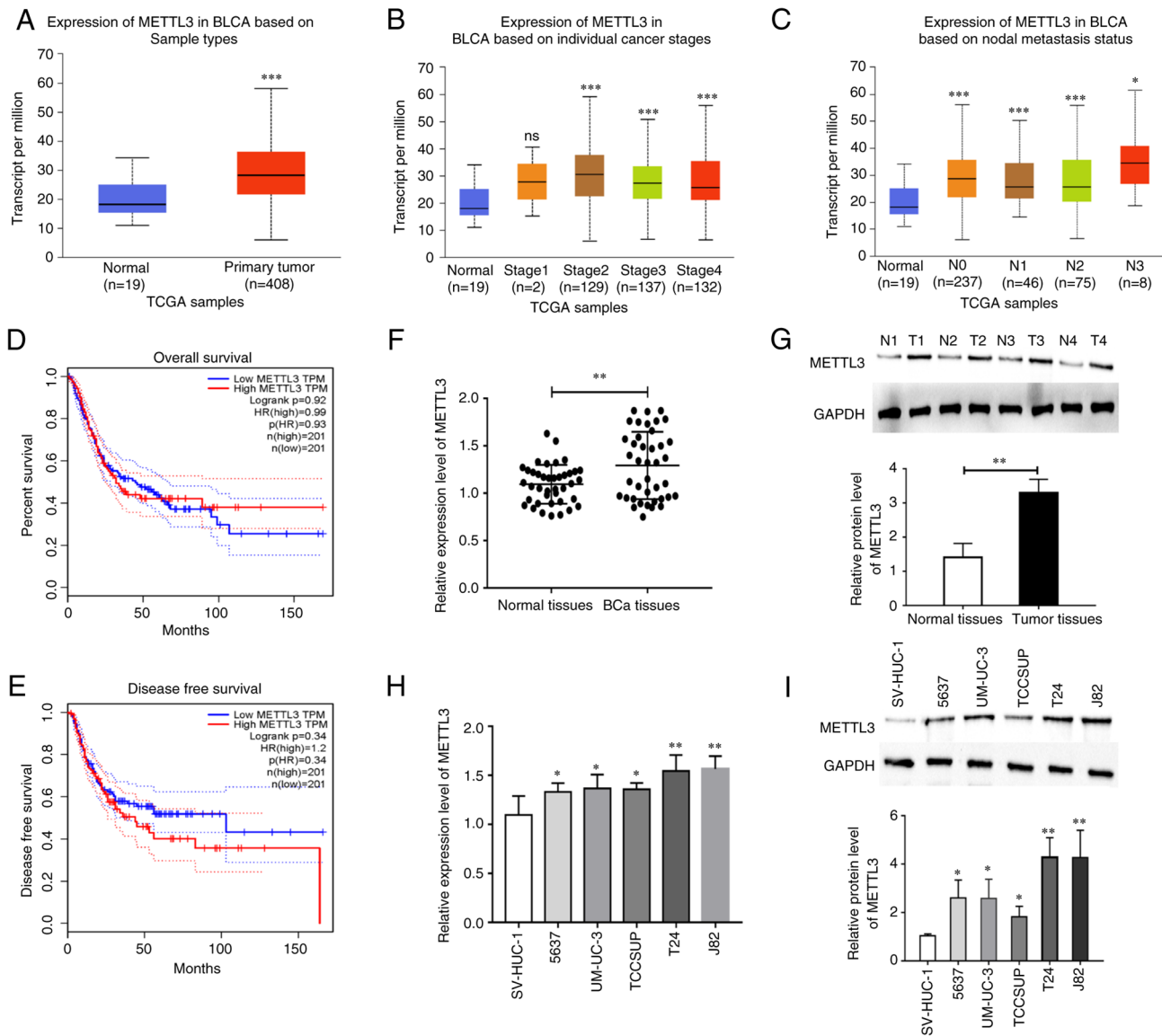


Figure 1. METTL3 is significantly overexpressed in BCa. (A) The expression of METTL3 was found to be significantly higher in BCa tumor tissues than in normal control tissues using TCGA database analysis. (B) The association of METTL3 expression levels with BCa cancer stages examined using TCGA database analysis. (C) The association of METTL3 expression levels with BCa nodal metastasis status. (D) No significant association was found between the METTL3 expression level and overall survival rate of patients with BCa using GEPIA database analysis. (E) No significant association was found between the METTL3 expression level and the disease-free survival rate of patients with BCa using GEPIA database analysis. (F) The mRNA expression of METTL3 in BCa tumor tissues was significantly higher than that in normal control tissues, as shown using RT-qPCR. (G) The protein expression of METTL3 in BCa tumor tissues was significantly higher than that in normal control tissues, as shown using western blot analysis. (H) The mRNA expression of METTL3 in BCa cells was significantly higher than that in normal control tissues, as shown using RT-qPCR. (I) The expression of METTL3 in BCa cells was significantly higher than that in normal control cells, as shown using western blot analysis. * $P < 0.05$, ** $P < 0.01$ and *** $P < 0.001$, vs. normal tissues or cells. ns, no significant difference; METTL3, methyltransferase-like 3; BCa, bladder cancer; TCGA, The Cancer Genome Atlas; RT-qPCR, reverse transcription-quantitative PCR.

prognosis of patients with BCa was analyzed. No significant association was observed between the METTL3 expression levels and the overall and disease-free survival of patients with BCa (Fig. 1D and E). The METTL3 expression levels were also verified in BCa and paraneoplastic tissues collected from Sir Run Run Hospital, Nanjing Medical University. As shown in Fig. 1F and G, the mRNA expression level of METTL3 was markedly higher in BCa tissues than in paraneoplastic tissues. Finally, the expression patterns of METTL3 were examined in BCa cells. The expression level of METTL3 was markedly higher in BCa cells. The most significant increase was observed in the T24 and J82 cells (Fig. 1H and I). These cell lines were thus used in subsequent assays.

Inhibition of METTL3 significantly suppresses BCa cell proliferation, migration and invasion. To investigate the biological effects of METTL3 in BCa, the expression level of METTL3 in BCa cells was decreased or increased by siRNA and an overexpression plasmid, respectively, and the transfection efficiency was verified using RT-qPCR and western blot analysis (Fig. S1). Cell proliferation was then examined using CCK-8 and EdU assays following the silencing of METTL3 expression in BCa cells. The results revealed that METTL3 siRNA significantly inhibited cell proliferation (Fig. 2A and B). Furthermore, METTL3 siRNA also inhibited cell migration and invasion, as shown by Transwell assay (Fig. 2C and D). In addition, the results of flow cytometry

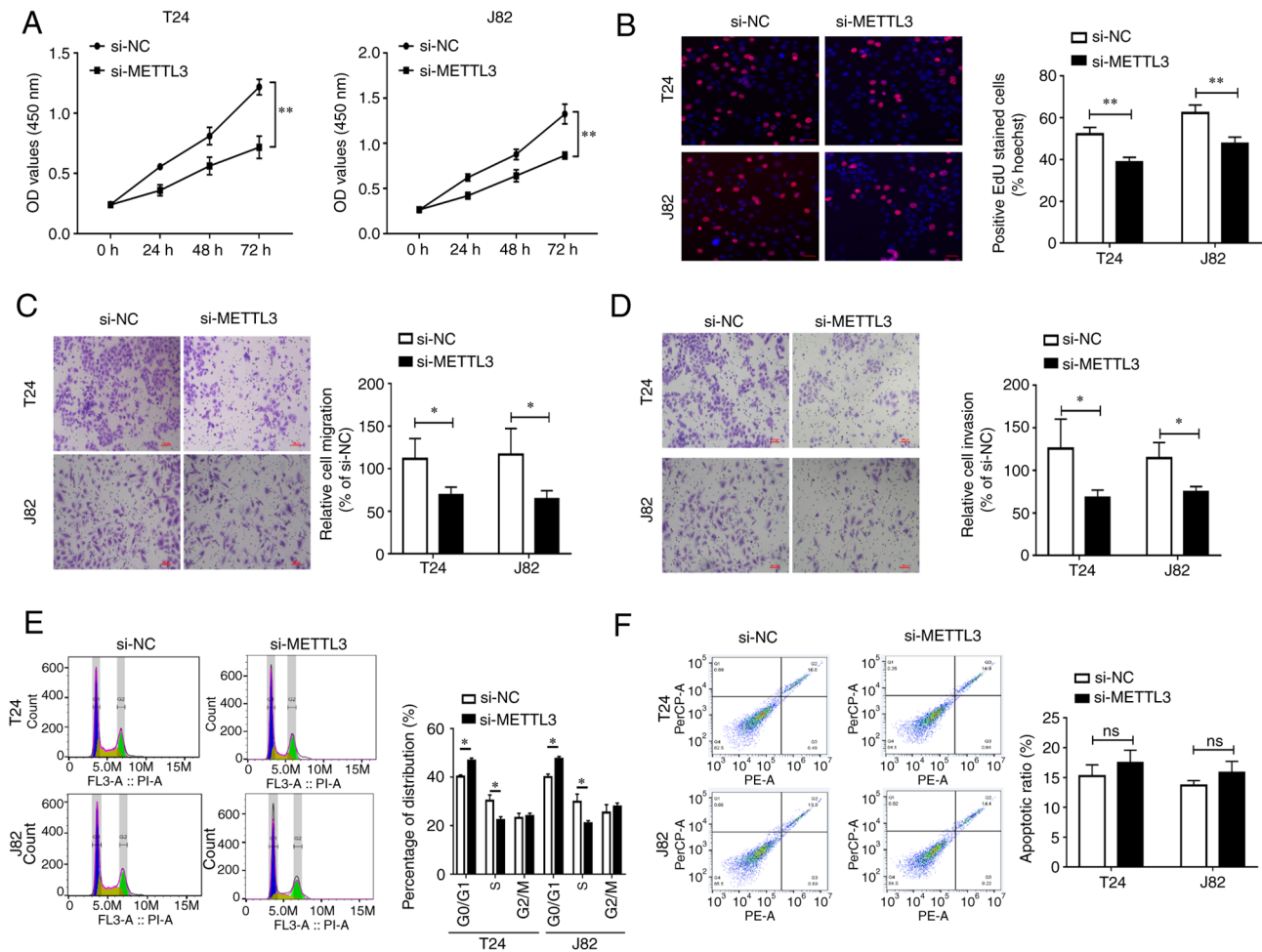


Figure 2. Inhibition of METTL3 significantly suppresses the proliferation, migration and invasion of BCa cells. (A) Detection of cell proliferation using Cell Counting Kit-8 assay after the silencing of METTL3 in BCa cells. (B) Detection of cell proliferation using EdU assay after the silencing of METTL3 in BCa cells. (C) Detection of cell migration using Transwell assay after the silencing of METTL3 in BCa cells. (D) Detection of cell invasion using Transwell assay after the silencing of METTL3 in BCa cells. (E and F) Detection of cell cycle and apoptosis using flow cytometry after the silencing of METTL3 in BCa cells. * $P < 0.05$ and ** $P < 0.01$. ns, no significant difference; METTL3, methyltransferase-like 3; BCa, bladder cancer; EdU, 5-ethynyl-2'-deoxyuridine.

revealed that the silencing METTL3 repressed the cell cycle, while no significant changes in the cell apoptotic ratio were observed after the silencing of METTL3 expression in BCa cells (Fig. 2E and F). In addition, cell phenotype changes were examined in BCa cells transfected with METTL3 overexpression plasmid using an *in vitro* assay, and it was found that the overexpression of METTL3 produced opposite biological effects (Fig. S2). These results indicated that METTL3 may function as an oncogene in BCa.

RRAS is a potential downstream target of METTL3. To explore the potential downstream targets of METTL3, potential genes that were highly correlated with METTL3 in the GEPIA database were screened (Table SIV). The expression of the potential genes was then analyzed in BCa tissues and only three genes exhibited a differential expression [low density lipoprotein receptor class A domain containing 2 (LDLRAD2), RRAS and proteasome 20S subunit beta 10 (PSMB10)]. LDLRAD2 has been reported to function as an oncogene in previous studies (25,26), while PSMB10 was upregulated in BCa tissues according to the results of the online database (GEPIA, <http://gepia.cancer-pku.cn/> and

UALCAN, <https://ualcan.path.uab.edu/>), which was inconsistent with the correlation with METTL3. Hence, RRAS was selected for further analysis. RRAS negatively correlated with METTL3 in BCa tissues (Fig. 3A). The analysis of the GEPIA database revealed that the expression of RRAS was significantly lower in BCa tissues than in normal control tissues (Fig. 3B). These findings suggest that METTL3 may negatively regulate the expression of RRAS. The METTL3 methyltransferase can regulate gene expression by regulating the level of m6A modification of genes. To verify this mechanism of the METTL3-regulated expression of RRAS, m6A modification sites in the coding sequence region of RRAS were identified through database analysis (Fig. 3C). The MeRIP assay revealed that the overexpression of METTL3 increased the m6A modification level of RRAS, while the silencing of METTL3 significantly decreased the m6A modification level of RRAS (Fig. 3D), which also confirmed the initial hypothesis. Further detection using RT-qPCR and western blot analysis revealed that the overexpression of METTL3 suppressed the mRNA and protein expression levels of RRAS, while the silencing of METTL3 produced the opposite result (Fig. 3E and F). The results of the dual-luciferase reporter gene assay indicated that

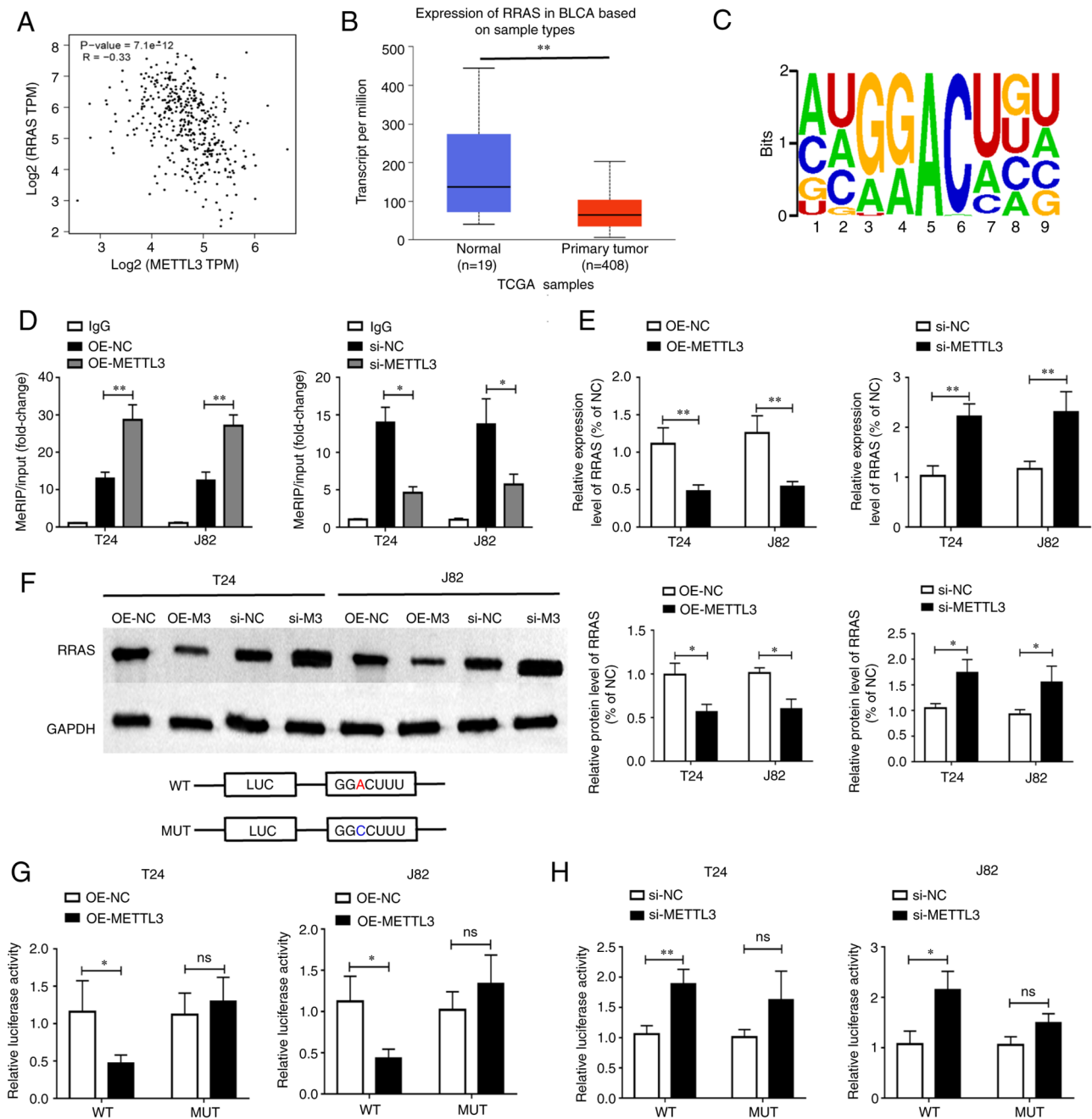


Figure 3. RRAS is a potential downstream target of METTL3. (A) A significant negative correlation between METTL3 and RRAS was found using GEPIA database analysis. (B) The expression of RRAS in BCa tumor tissues was found to be significantly lower than that in normal control tissues using TCGA database analysis. (C) The presence of m6A modification sites in the coding sequence region of RRAS was found using database analysis. (D) The level of m6A modification of RRAS was found to be significantly lower by MeRIP assay. MeRIP assay revealed that the overexpression of METTL3 increased the m6A modification level of RRAS, while the silencing of METTL3 significantly decreased the m6A modification level of RRAS. (E and F) Reverse transcription-quantitative PCR and western blot assays revealed that the overexpression of METTL3 inhibited the mRNA and protein expression levels of RRAS. (G and H) Dual luciferase reporter gene assays revealed that the overexpression of METTL3 inhibited the transcriptional activity of RRAS, while the silencing of METTL3 significantly increased the transcriptional activity of RRAS. * $P < 0.05$ and ** $P < 0.01$. ns, no significant difference; METTL3, methyltransferase-like 3; BCa, bladder cancer; GEPIA, Gene Expression Profiling Interactive Analysis; TCGA, The Cancer Genome Atlas; RRAS, RAS related; m6A, N6-methyladenosine; MeRIP, Magna methylated RNA immunoprecipitation.

the overexpression of METTL3 suppressed the transcriptional activity of RRAS in an m6A-dependent manner, while the silencing of METTL3 resulted in a significant increase in the transcriptional activity of RRAS (Fig. 3G and H). These experimental results indicate that METTL3 may inhibit RRAS expression by elevating the level of m6A modification of RRAS.

Silencing of METTL3 significantly inhibits tumor growth. To confirm the effects of METTL3 on tumor growth, a T24 cell line (LV-shMETTL-T24) with a stable low expression of METTL3 was constructed and injected into nude mice. The tumorigenic potential in mice in the LV-shMETTL3 group was significantly diminished compared with that of mice in the LV-NC group (Fig. 4A-C). This finding suggested

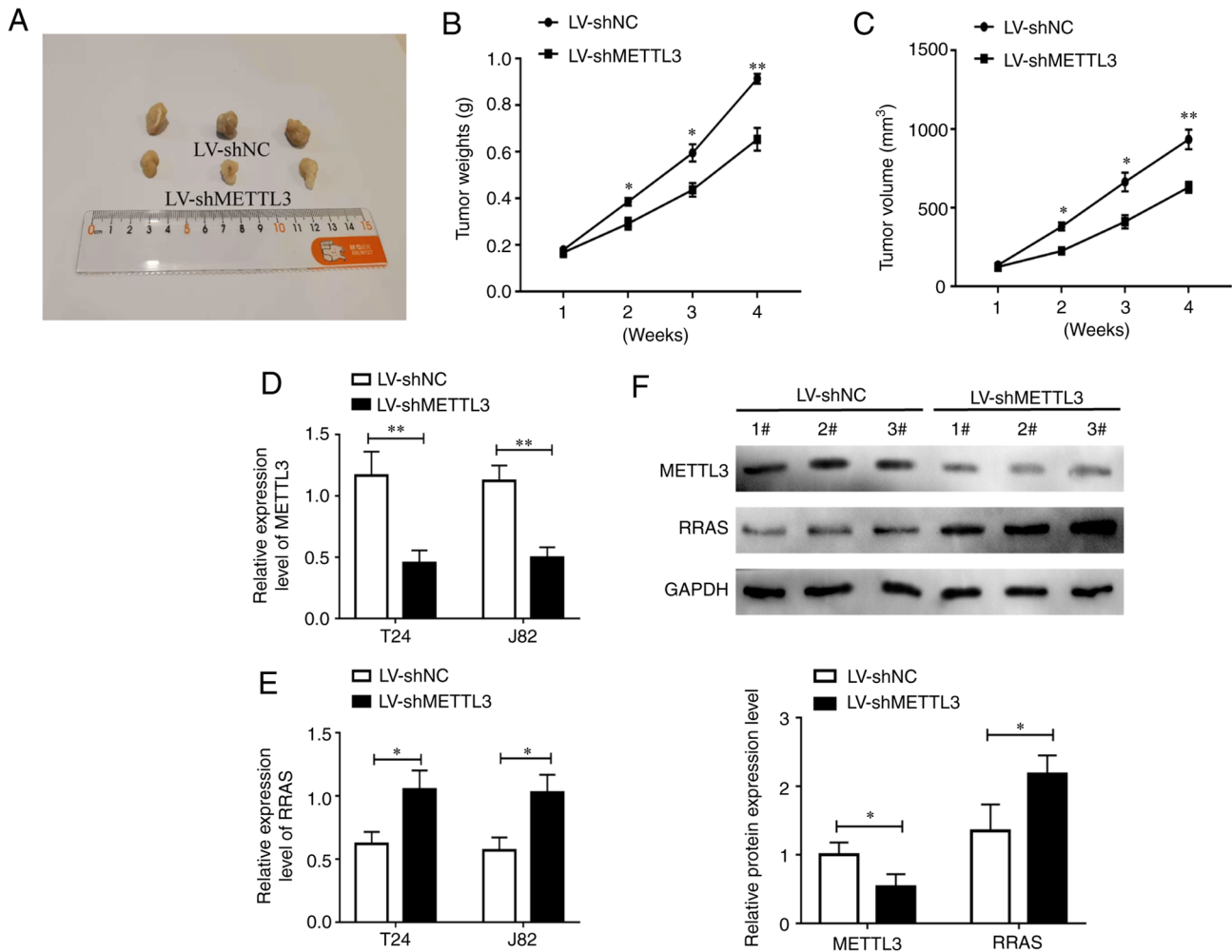


Figure 4. Silencing of METTL3 significantly inhibits tumor growth. (A) Silencing of METTL3 effectively decreased bladder cancer subcutaneous tumor growth. (B) The tumor weight was significantly decreased following the silencing of METTL3. (C) The tumor volume markedly decreased following the silencing of METTL3. (D-F) Reverse transcription-quantitative PCR and western blot analysis revealed that the silencing of METTL3 inhibited the mRNA and protein expression levels of RRAS in tumor tissues. * $P < 0.05$ and ** $P < 0.01$. METTL3, methyltransferase-like 3; RRAS, RAS related.

that METTL3 functions as a pro-oncogenic factor in BCa. Furthermore, the expression levels of METTL3 and RRAS were examined using RT-qPCR and western blot analysis. The results revealed that LV-shMETTL3 suppressed the expression level of METTL3, while it promoted RRAS expression at both the mRNA and protein level (Fig. 4D-F).

Overexpression of RRAS suppresses BCa cell proliferation, migration and invasion. To explore the biological role of RRAS in BCa, the expression level of RRAS and METTL3 was increased in BCa cells using an overexpression plasmid and the cell proliferative, migratory and invasive abilities were examined using EdU and Transwell assays. The results demonstrated that the overexpression of RRAS significantly inhibited cell proliferation, migration and invasion, while the co-overexpression of METTL3 partially attenuated the inhibitory effects of RRAS overexpression (Fig. 5). These results demonstrate that RRAS may function as a tumor suppressor in BCa tissues.

YTHDF2 preferentially binds to the m6A sites of RRAS. In order to examine the potential m6A recognition processes that can identify RRAS, the correlation between the expression

levels of all m6A recognition proteins and RRAS was analyzed in BCa tissues. The results revealed that IGF2BP2, IGF2BP3, YTHDC1, YTHDC2, YTHDF1 and YTHDF2 exhibited a significant correlation with RRAS (Fig. S3). The expression levels of these m6A recognition proteins in BCa were then analyzed. The expression of levels IGF2BP3, YTHDF1 and YTHDF2 were significantly increased, while the expression of YTHDC1 was significantly decreased in BCa tissues (Fig. S4). IGF2BP3 can recruit RNA stabilizers (27), YTHDF1 can facilitate mRNA translation efficiency (28), and YTHDC1 can recruit the RNA splicing and control the nuclear export (29). These biological functions are inconsistent with their expression levels and the reduced expression level of RRAS. YTHDF2 can promote mRNA degradation and decrease gene expression (30-32), which may be the reason for the decrease in RRAS expression. Therefore, YTHDF2 was selected for further analysis. The expression levels of YTHDF2 negatively correlated with RRAS expression (Fig. 6A). Further analysis revealed that the m6A modification site of RRAS was located within the YTHDF2 protein binding site region (Fig. 6B). The RIP assay revealed the binding of the YTHDF2 protein to RRAS in BCa cells, indicating that YTHDF2 can bind the

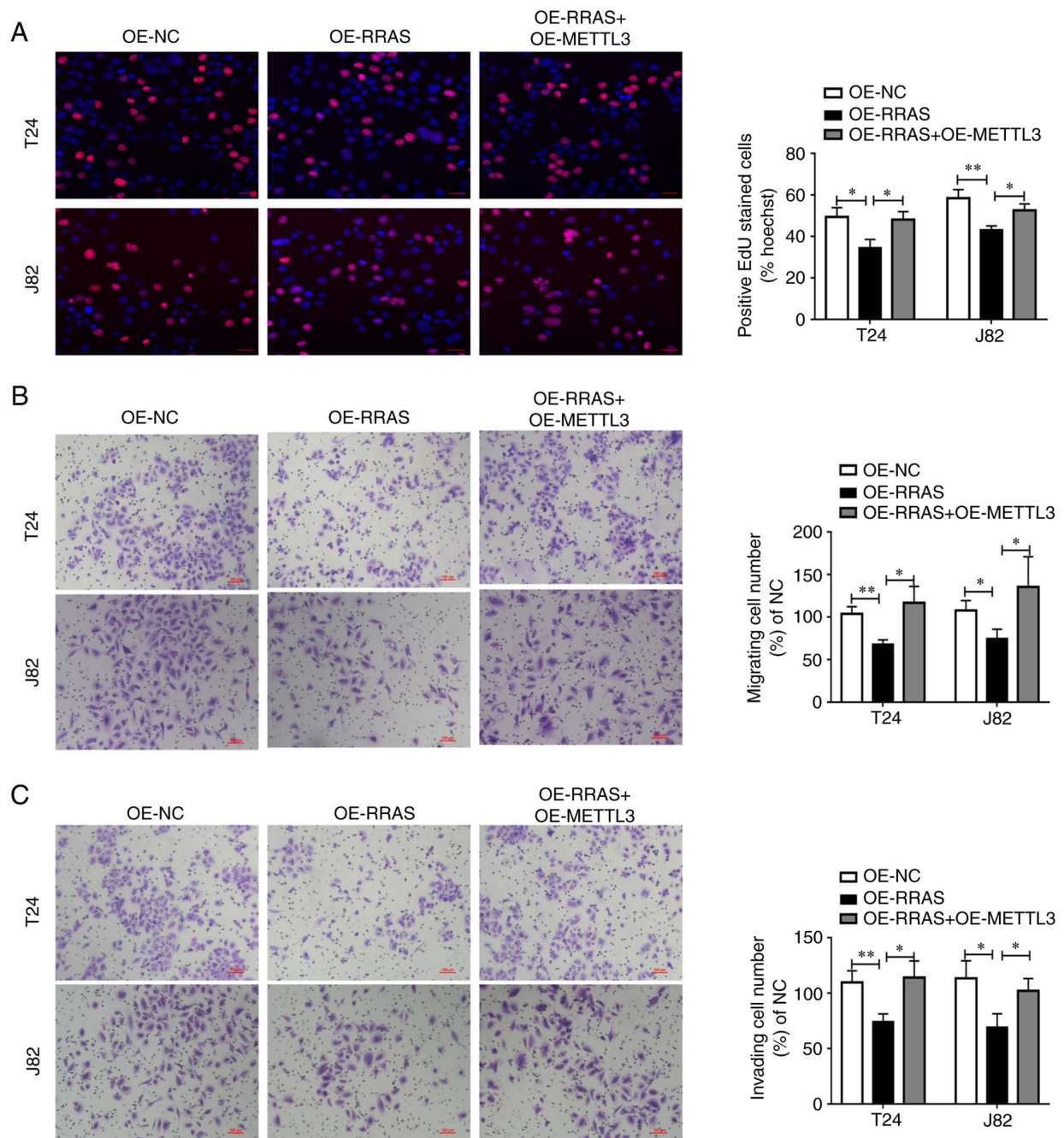


Figure 5. Overexpression of RRAS markedly inhibits cell proliferation, migration and invasion. (A) Detection of cell proliferation using EdU assay following the overexpression of RRAS and METTL3 in BCa cells. (B) Detection of cell migration using Transwell assay following the overexpression of RRAS and METTL3 in BCa cells. (C) Detection of cell invasion using Transwell assay following the overexpression of RRAS and METTL3 in BCa cells. * $P < 0.05$ and ** $P < 0.01$. RRAS, RAS related; EdU, 5-ethynyl-2'-deoxyuridine; METTL3, methyltransferase-like 3; BCa, bladder cancer; OE, overexpression.

m6A modification site of RRAS (Fig. 6C). The overexpression of YTHDF2, as verified using RT-qPCR and western blot analysis, inhibited the mRNA and protein expression levels of RRAS, while the silencing of YTHDF2 produced the opposite results (Fig. 6D and E). These results suggest that YTHDF2 may be able to bind the m6A modification site of RRAS and lead to the degradation of RRAS mRNA.

Discussion

The main reason for the high mortality rate of patients with BCa is the recurrence and metastasis that occurs in some patients,

even following treatment with conventional regimens (33,34). The mechanisms that are involved are complex. The molecular staging of BCa is still exploratory. Several staging schemes have been proposed based on different research directions. These schemes are currently mainly used in the prognostic assessment of the therapeutic sensitivity of targeted chemotherapy and immune drugs (35,36). The lack of in-depth research on pathogenesis and difficulties in the development of new drugs and technology have prevented significant progress being made in research on systemic treatment and early diagnostic methods for BCa in the past decades. There is an urgent need to identify new therapeutic targets for bladder muscle cancer. Further in-depth

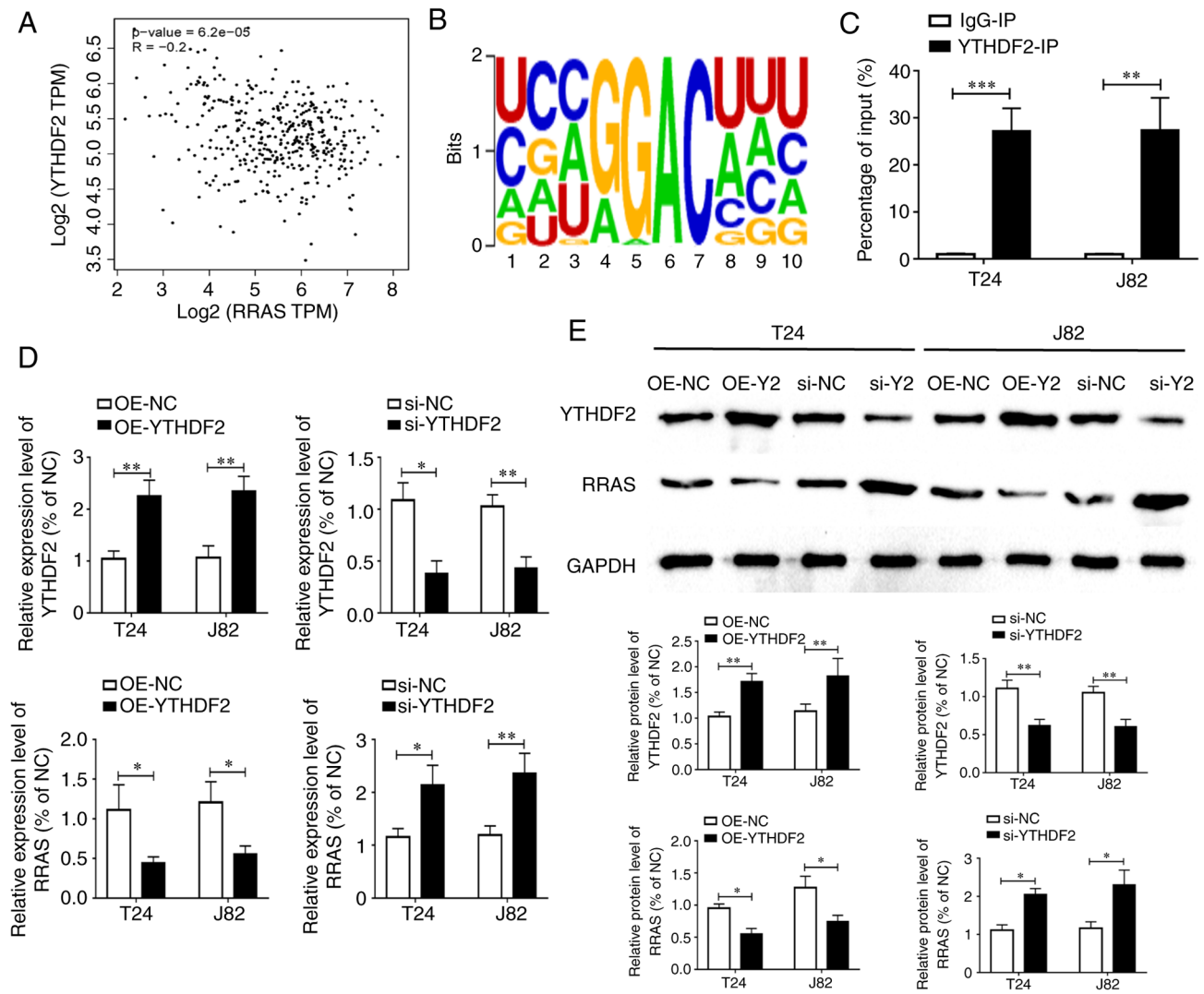


Figure 6. YTHDF2 preferentially decodes the m6A residue of RRAS. (A) YTHDF2 was found to exhibit a significant negative correlation with RRAS using Gene Expression Profiling Interactive Analysis database analysis. (B) The RRAS m6A modification site was exactly in the YTHDF2 protein binding region. (C) RNA Immunoprecipitation-qPCR was conducted to confirm the RRAS mRNA enrichment by YTHDF2 in bladder cancer cells. (D and E) The overexpression of YTHDF2 was found to promote the mRNA and protein expression levels of YTHDF2 using reverse transcription-quantitative PCR and western blot analysis, while the silencing of YTHDF2 produced the opposite results. Moreover, the upregulation of YTHDF2 suppressed the mRNA and protein expression levels of RRAS, while the suppression of YTHDF2 produced the opposite results. * $P < 0.05$, ** $P < 0.01$ and *** $P < 0.001$. YTHDF2, YTH N6-methyladenosine RNA binding protein 2; METTL3, methyltransferase-like 3; N⁶-methyladenosine; OE, overexpression.

studies on the molecular mechanisms associated with BCa progression and metastasis are of utmost importance.

m6A is the most common and abundant mRNA modification in eukaryotic mRNAs and lncRNAs (14). Numerous *in vitro* data have established the involvement of m6A modifications in multiple aspects affecting mRNA metabolism, including RNA splicing, processing, translocation, stability and translation (16). m6A modifications are involved in regulating mRNA splicing, nuclear export, mRNA stability, translation and miRNA processing (37,38). The wide range of m6A modifications has led to their involvement in a variety of physiological and pathological processes, such as cancer and immune responses (39,40). Previous studies have also demonstrated that m6A modifications are closely associated with the development and progression of BCa. Fine particulate matter induces the METTL3-mediated m6A modification of BIRC5 mRNA in BCa, leading to malignant tumor progression (41).

The JNK signaling axis promotes the BCa immune escape by regulating METTL3-mediated m6A modification of PD-L1 mRNA (42). circ0008399 promotes m6A modification by interacting with ALKBH5, which inhibits cell proliferation and sensitizes BCa cells to cisplatin through m6A-CK2 α -mediated glycolysis (43). However, the molecular mechanisms and biological effects of m6A modification in BCa warrant further investigation.

The present study, to the best of our knowledge, provides the first evidence from bioinformatics analysis and assay validation that METTL3 expression is significantly increased in BCa tissues and demonstrates a strong association between high METTL3 expression and BCa staging and staging. However, no significant association was found between the METTL3 expression levels and the prognosis of patients with BCa. The patients with BCa were not followed-up for 5 years and thus the data from Sir Run Run Hospital, Nanjing

Medical University were not analyzed. The long-term importance of the findings of the present study will be explored in future studies. Furthermore, the *ex vivo* experimental results indicated that METTL3 may play a role as a pro-cancer factor in BCa by promoting cell proliferation, migration and invasion. The bioinformatics analysis suggested RRAS as a potential downstream target of METTL3. RRAS has important biological roles in breast cancer (44), gastric cancer (45), colorectal cancer (46) and melanoma (47). However, its role in BCa remains unclear. Mechanistic analyses in the present study indicated that METTL3 may inhibit the expression of RRAS by increasing its m6A modification level. YTHDF2 was the first specific m6A recognition protein identified to regulate mRNA degradation (48,49). YTHDF2 also plays an integral role in tumorigenesis and malignant progression (50,51). Evidence provided in the present study indicates that YTHDF2 may bind to the m6A modification site of RRAS and lead to the degradation of RRAS mRNA.

There are several limitations to the present study. First, the present study did not include a sufficient number of clinical specimens and detailed clinical information to further explore the diagnostic efficacy of METTL3. The authors aim to address this limitation in future research. Second, while the results confirmed that METTL3 promotes tumor cell migration and invasion, these findings were not validated *in vivo*. Of note, the possible downstream targets of METTL3 were not screened by m6A sequencing and high-throughput sequencing, which limits the innovation of the study renders the findings unconvincing. Moreover, the underlying mechanism of METTL3 upregulation was not investigated in the present study. Ni *et al* (42) demonstrated that JNK signaling was associated with an increased METTL3 expression in BCa. In addition, Liu *et al* (41) identified that PM2.5 may enhance the expression of METTL3 by inducing the promoter hypomethylation of its promoter and increasing the binding affinity of the transcription factor HIF1A. Due to the limitations regarding time and resources, the present study not explore and verify the mechanisms for the increase of METTL3. In the future, the authors aim to explore the potential mechanism for the increase of METTL3 in BCa cells.

In conclusion, the findings of the present study indicate that METTL3 expression is significantly increased in BCa. METTL3 may contribute to the malignant progression of BCa by regulating the RRAS/YTHDF2 signaling axis, thus promoting cell proliferation, migration and invasion.

Acknowledgements

Not applicable.

Funding

The present study was supported by the Science and Technology Development Fund of Nanjing Medical University (grant no. NMUB2019084).

Availability of data and materials

The datasets used and/or analyzed during the current study are available from the corresponding author on reasonable request.

Authors' contributions

SZ, DMC, JXC and XLX were involved in the conceptualization of the study, as well as in the study methodology, and in the writing, reviewing and editing of the manuscript. DW and YX were involved in the investigative aspects of the study, as well as in data curation, and in the writing and preparation of the original draft. SZ, JXC and XLX were involved in visualization, data validation, supervision and in the provision of software. JXC and XLX confirm the authenticity of all the raw data. All authors have read and approved the final manuscript.

Ethics approval and consent to participate

The research protocol conformed to the principles outlined in the Declaration of Helsinki. All patients provided written informed consent and the protocol of the study was approved by the Research Ethics Committee of Sir Run Run Hospital, Nanjing Medical University. The animal experiment was approved (approval no. 2021-AR-008) and monitored by the Animal Ethics Committee of Sir Run Run Hospital, Nanjing Medical University.

Patient consent for publication

Not applicable.

Competing interests

The authors declare that they have no competing interests.

References

1. Tran L, Xiao JF, Agarwal N, Duex JE and Theodorescu D: Advances in bladder cancer biology and therapy. *Nat Rev Cancer* 21: 104-121, 2021.
2. Lenis AT, Lec PM, Chamie K and Mshs MD: Bladder cancer: A review. *JAMA* 324: 1980-1991, 2020.
3. Patel VG, Oh WK and Galsky MD: Treatment of muscle-invasive and advanced bladder cancer in 2020. *CA Cancer J Clin* 70: 404-423, 2020.
4. Joensen UN, Maibom SL and Poulsen AM: Surgical management of muscle invasive bladder cancer: A review of current recommendations. *Semin Oncol Nurs* 37: 151104, 2021.
5. Witjes JA, Bruins HM, Cathomas R, Compérat EM, Cowan NC, Gakis G, Hernández V, Linares Espinós E, Lorch A, Neuzillet Y, *et al*: European association of urology guidelines on muscle-invasive and metastatic bladder cancer: Summary of the 2020 guidelines. *Eur Urol* 79: 82-104, 2021.
6. Nason GJ, Ajib K, Tan GH and Kulkarni GS: Bladder-sparing treatment options in localized muscle-invasive bladder cancer. *Expert Rev Anticancer Ther* 20: 179-188, 2020.
7. Nadal R and Bellmunt J: Management of metastatic bladder cancer. *Cancer Treat Rev* 76: 10-21, 2019.
8. Alifrangis C, McGovern U, Freeman A, Powles T and Linch M: Molecular and histopathology directed therapy for advanced bladder cancer. *Nat Rev Urol* 16: 465-483, 2019.
9. Jordan B and Meeks JJ: T1 bladder cancer: Current considerations for diagnosis and management. *Nat Rev Urol* 16: 23-34, 2019.
10. Jia J, Wu S, Jia Z, Wang C, Ju C, Sheng J, He F, Zhou M and He J: Novel insights into m⁶A modification of coding and non-coding RNAs in tumor biology: From molecular mechanisms to therapeutic significance. *Int J Biol Sci* 18: 4432-4451, 2022.
11. Chen J, Fang Y, Xu Y and Sun H: Role of m⁶A modification in female infertility and reproductive system diseases. *Int J Biol Sci* 18: 3592-3604, 2022.

12. Qu X, Zhang Y, Sang X, Ren D, Zhao H and Wong STC: Methyladenosine modification in RNAs: From regulatory roles to therapeutic implications in cancer. *Cancers (Basel)* 14: 3195, 2022.
13. Zhang F, Liu H, Duan M, Wang G, Zhang Z, Wang Y, Qian Y, Yang Z and Jiang X: Crosstalk among m⁶A RNA methylation, hypoxia and metabolic reprogramming in TME: From immunosuppressive microenvironment to clinical application. *J Hematol Oncol* 15: 84, 2022.
14. Murakami S and Jaffrey SR: Hidden codes in mRNA: Control of gene expression by m⁶A. *Mol Cell* 82: 2236-2251, 2022.
15. Shi B, Liu WW, Yang K, Jiang GM and Wang H: The role, mechanism, and application of RNA methyltransferase METTL14 in gastrointestinal cancer. *Mol Cancer* 21: 163, 2022.
16. Shen D, Wang B, Gao Y, Zhao L, Bi Y, Zhang J, Wang N, Kang H, Pang J, Liu Y, *et al*: Detailed resume of RNA m⁶A demethylases. *Acta Pharm Sin B* 12: 2193-2205, 2022.
17. Chen D, Cheung H, Lau HC, Yu J and Wong CC: N⁶-methyladenosine RNA-binding protein YTHDF1 in gastrointestinal cancers: Function, molecular mechanism and clinical implication. *Cancers (Basel)* 14: 3489, 2022.
18. Wu X, Ye W and Gong Y: The role of RNA methyltransferase METTL3 in normal and malignant hematopoiesis. *Front Oncol* 12: 873903, 2022.
19. Li E, Xia M, Du Y, Long K, Ji F, Pan F, He L, Hu Z and Guo Z: METTL3 promotes homologous recombination repair and modulates chemotherapeutic response in breast cancer by regulating the EGF/RAD51 axis. *Elife* 11: e75231, 2022.
20. Zhu Y, Peng X, Zhou Q, Tan L, Zhang C, Lin S and Long M: METTL3-mediated m⁶A modification of STEAP2 mRNA inhibits papillary thyroid cancer progress by blocking the Hedgehog signaling pathway and epithelial-to-mesenchymal transition. *Cell Death Dis* 13: 358, 2022.
21. Li H, Wang C, Lan L, Yan L, Li W, Evans I, Ruiz EJ, Su Q, Zhao G, Wu W, *et al*: METTL3 promotes oxaliplatin resistance of gastric cancer CD133+ stem cells by promoting PARP1 mRNA stability. *Cell Mol Life Sci* 79: 135, 2022.
22. Han J, Wang JZ, Yang X, Yu H, Zhou R, Lu HC, Yuan WB, Lu JC, Zhou ZJ, Lu Q, *et al*: METTL3 promote tumor proliferation of bladder cancer by accelerating pri-miR221/222 maturation in m⁶A-dependent manner. *Mol Cancer* 18: 110, 2019.
23. Cheng M, Sheng L, Gao Q, Xiong Q, Zhang H, Wu M, Liang Y, Zhu F, Zhang Y, Zhang X, *et al*: The m⁶A methyltransferase METTL3 promotes bladder cancer progression via AFB4/NF- κ B/MYC signaling network. *Oncogene* 38: 3667-3680, 2019.
24. Livak KJ and Schmittgen TD: Analysis of relative gene expression data using real-time quantitative PCR and the 2(-Delta Delta C(T)) method. *Methods* 25: 402-408, 2001.
25. Wei Y, Zhang F, Zhang T, Zhang Y, Chen H, Wang F and Li Y: LDLRAD2 overexpression predicts poor prognosis and promotes metastasis by activating Wnt/ β -catenin/EMT signaling cascade in gastric cancer. *Aging (Albany NY)* 11: 8951-8968, 2019.
26. Li J, Huang W, Han Q, Xiong J and Song Z: LDLRAD2 promotes pancreatic cancer progression through Akt/mTOR signaling pathway. *Med Oncol* 38: 2, 2021.
27. Wan W, Ao X, Chen Q, Yu Y, Ao L, Xing W, Guo W, Wu X, Pu C, Hu X, *et al*: MEMETTL3/IGF2BP3 axis inhibits tumor immune surveillance by upregulating N⁶-methyladenosine modification of PD-L1 mRNA in breast cancer. *Mol Cancer* 21: 60, 2022.
28. Xia H, Wu Y, Zhao J, Cheng C, Lin J, Yang Y, Lu L, Xiang Q, Bian T and Liu Q: N⁶-methyladenosine-modified circSAV1 triggers ferroptosis in COPD through recruiting YTHDF1 to facilitate the translation of IREB2. *Cell Death Differ*: Feb 24, 2023 (Epub ahead of print).
29. Timcheva K, Dufour S, Touat-Todeschini L, Burnard C, Carpentier MC, Chuffart F, Merret R, Helsmoortel M, Ferré S, Grézy A, *et al*: Chromatin-associated YTHDC1 coordinates heat-induced reprogramming of gene expression. *Cell Rep* 41: 111784, 2022.
30. Hu L, Yu Y, Shen Y, Huang H, Lin D, Wang K, Yu Y, Li K, Cao Y, Wang Q, *et al*: Ythdf2 promotes pulmonary hypertension by suppressing Hmox1-dependent anti-inflammatory and antioxidant function in alveolar macrophages. *Redox Biol* 61: 102638, 2023.
31. Yang Y, Yan Y, Yin J, Tang N, Wang K, Huang L, Hu J, Feng Z, Gao Q and Huang A: O-GlcNAcylation of YTHDF2 promotes HBV-related hepatocellular carcinoma progression in an N⁶-methyladenosine-dependent manner. *Signal Transduct Target Ther* 8: 63, 2023.
32. Zhuang M, Geng X, Han P, Che P, Liang F, Liu C, Yang L, Yu J, Zhang Z, Dong W and Ji SJ: YTHDF2 in dentate gyrus is the m⁶A reader mediating m⁶A modification in hippocampus-dependent learning and memory. *Mol Psychiatry*: Jan 20, 2023 (Epub ahead of print).
33. Martin A, Woolbright BL, Umar S, Ingersoll MA and Taylor JA III: Bladder cancer, inflammaging and microbiomes. *Nat Rev Urol* 19: 495-509, 2022.
34. Lee YC, Lam HM, Rosser C, Theodorescu D, Parks WC and Chan KS: The dynamic roles of the bladder tumour microenvironment. *Nat Rev Urol* 19: 515-533, 2022.
35. Liu S, Chen X and Lin T: Emerging strategies for the improvement of chemotherapy in bladder cancer: Current knowledge and future perspectives. *J Adv Res* 39: 187-202, 2022.
36. Ranti D, Bieber C, Wang YS, Sfakianos JP and Horowitz A: Natural killer cells: Unlocking new treatments for bladder cancer. *Trends Cancer* 8: 698-710, 2022.
37. Li Y, Meng L and Zhao B: The roles of N⁶-methyladenosine methylation in the regulation of bone development, bone remodeling and osteoporosis. *Pharmacol Ther* 238: 108174, 2022.
38. Zhuo R, Xu M, Wang X, Zhou B, Wu X, Leone V, Chang EB and Zhong X: The regulatory role of N⁶-methyladenosine modification in the interaction between host and microbes. *Wiley Interdiscip Rev RNA* 13: e1725, 2022.
39. Zhou H, Mao L, Xu H, Wang S and Tian J: The functional roles of m⁶A modification in T lymphocyte responses and autoimmune diseases. *Cytokine Growth Factor Rev* 65: 51-60, 2022.
40. Li X, Ma S, Deng Y, Yi P and Yu J: Targeting the RNA m⁶A modification for cancer immunotherapy. *Mol Cancer* 21: 76, 2022.
41. Liu H, Gu J, Huang Z, Han Z, Xin J, Yuan L, Du M, Chu H, Wang M and Zhang Z: Fine particulate matter induces METTL3-mediated m⁶A modification of BIRC5 mRNA in bladder cancer. *J Hazard Mater* 437: 129310, 2022.
42. Ni Z, Sun P, Zheng J, Wu M, Yang C, Cheng M, Yin M, Cui C, Wang G, Yuan L, *et al*: JNK signaling promotes bladder cancer immune escape by regulating METTL3-mediated m⁶A modification of PD-L1 mRNA. *Cancer Res* 82: 1789-1802, 2022.
43. Yu H, Yang X, Tang J, Si S, Zhou Z, Lu J, Han J, Yuan B, Wu Q, Lu Q and Yang H: ALKBH5 inhibited cell proliferation and sensitized bladder cancer cells to cisplatin by m⁶A-CK2 α -mediated glycolysis. *Mol Ther Nucleic Acids* 23: 27-41, 2020.
44. Li H, Prever L, Hsu MY, Lo WT, Margaria JP, De Santis MC, Zanini C, Forni M, Novelli F, Pece S, *et al*: Phosphoinositide conversion inactivates R-RAS and drives metastases in breast cancer. *Adv Sci (Weinh)* 9: e2103249, 2022.
45. Hu Q, Masuda T, Koike K, Sato K, Tobo T, Kuramitsu S, Kitagawa A, Fujii A, Noda M, Tsuruda Y, *et al*: Oxysterol binding protein-like 3 (OSBPL3) is a novel driver gene that promotes tumor growth in part through R-Ras/Akt signaling in gastric cancer. *Sci Rep* 11: 19178, 2021.
46. Raza A, Pandey MS, Jin Q and Mulder KM: km23-1/DYNLRB1 regulation of MEK/ERK signaling and R-Ras in invasive human colorectal cancer cells. *Cell Biol Int* 44: 155-165, 2020.
47. Sung H, Kanchi KL, Wang X, Hill KS, Messina JL, Lee JH, Kim Y, Dees ND, Ding L, Teer JK, *et al*: Inactivation of RASA1 promotes melanoma tumorigenesis via R-Ras activation. *Oncotarget* 7: 23885-23896, 2016.
48. Liu R, Jia Y, Kong G and He A: Novel insights into roles of N⁶-methyladenosine reader YTHDF2 in cancer progression. *J Cancer Res Clin Oncol* 148: 2215-2230, 2022.
49. Lee Y, Choe J, Park OH and Kim YK: Molecular mechanisms driving mRNA degradation by m⁶A modification. *Trends Genet* 36: 177-188, 2020.
50. Chen X, Zhou X and Wang X: m⁶A binding protein YTHDF2 in cancer. *Exp Hematol Oncol* 11: 21, 2022.
51. Wang JY and Lu AQ: The biological function of m⁶A reader YTHDF2 and its role in human disease. *Cancer Cell Int* 21: 109, 2021.

